



Brazilian Journal of Physics

ISSN: 0103-9733

luizno.bjp@gmail.com

Sociedade Brasileira de Física  
Brasil

Pires, L. F.; Arthur, R. C. J.; Bacchi, O. O. S.; Reichardt, K.  
Representative Gamma-ray Computed Tomography Calibration for Applications in Soil Physics  
Brazilian Journal of Physics, vol. 41, núm. 1, mayo, 2011, pp. 21-28  
Sociedade Brasileira de Física  
São Paulo, Brasil

Available in: <http://www.redalyc.org/articulo.oa?id=46421597004>

- How to cite
- Complete issue
- More information about this article
- Journal's homepage in redalyc.org

redalyc.org

Scientific Information System  
Network of Scientific Journals from Latin America, the Caribbean, Spain and Portugal  
Non-profit academic project, developed under the open access initiative

# Representative Gamma-ray Computed Tomography Calibration for Applications in Soil Physics

L. F. Pires · R. C. J. Arthur · O. O. S. Bacchi · K. Reichardt

Received: 27 July 2010 / Published online: 7 April 2011  
© Sociedade Brasileira de Física 2011

**Abstract** Tomographic image quality in soil physics applications is extremely dependent on calibration. Here, good calibrations of the system are necessary to avoid errors during soil evaluations by computed tomography (CT), which can hamper interpretations of physical parameters of the soil. In order to analyze the relevance of a good calibration curve (CC) for measurements of soil physical properties, determinations of soil bulk density ( $\rho_b$ ) were obtained using four different CCs established for a homemade CT scanner dedicated especially to soil physics. The calibrations of the system were obtained through the relationship between tomographic units and corresponding linear attenuation coefficients ( $\mu_1$ ) of different materials. Data show that different calibration curves produce distinct  $\rho_b$  values affecting the quality of results of this soil physical property when evaluated by CT. However, it was demonstrated that even using non-homogeneous materials for CT calibration the results of  $\rho_b$  practically are of the same order of magnitude of the whole system error estimated in  $0.05 \text{ g cm}^{-3}$  (taking the water as reference).

**Keywords** Gamma-ray attenuation · Soil bulk density · Tomographic unit · Radioisotope application · Applied nuclear physics

## 1 Introduction

Computed tomography (CT) using X- and gamma-rays has been largely used in medicine since the 1970s. CT is a non-destructive imaging technique that allows 2-D and 3-D characterization of high-quality images of different materials with a good resolution. The method is based on the computation of a large number of transmission measurements of a photon beam used to reconstruct images cross-sections of scanned materials [1]. Due to the existence of a strong linear bivariate relationship between Hounsfield units and the material density, it is possible to obtain quantitative analysis of this physical property inside 2-D and 3-D CT images [2].

Beyond this application in modern medicine, applications of CT have occurred in different agronomic studies since 1982. Crestana et al. [3–5] showed the characteristics and possible uses of a very inexpensive, homemade CT scanner dedicated specially to soil physics. Phogat and Aylmore [6] made direct measurements of the spatial distribution of soil macroporosity. Macedo et al. [7] presented a CT scanner and a methodology for soil investigation at the microscale. Clausnitzer and Hopmans [2] proposed a method to determine the phase-volume fractions in tomographic representations of two-phase systems. Jégou et al. [8] evaluated the impact of soil compaction due to machinery traffic in the field on earthworm burrow systems. Pires et al. [9, 10] measured the range of the influence of tensiometer and solution extractor porous cups, its response power, and its operation in soil physical measurements and in another paper presented the use of 2-D tomographic images for the evaluation of the effect of core sampling devices in soil structure. Oliveira

---

L. F. Pires (✉)  
Laboratory of Soil Physics and Environmental Sciences,  
Department of Physics, State University of Ponta Grossa  
(UEPG), 84.030-900, Ponta Grossa, PR, Brazil  
e-mail: lfp@uepg.br, luizfpires@gmail.com

R. C. J. Arthur · O. O. S. Bacchi · K. Reichardt  
Laboratory of Soil Physics, Center for Nuclear Energy  
in Agriculture, The University of São Paulo, 13.400-970,  
Piracicaba, SP, Brazil

et al. [11] presented the development and applications of 3-D gamma-ray tomography system using ray casting volume rendering techniques.

To reliably determine soil physical parameters using CT images, one needs good calibrations of the system [3–5]. Problems during curve calibration evaluation can lead to under or overestimations of the soil physical property to be analyzed. These errors can also hamper interpretations of physical parameters of the soil, primarily those related to water transport important for practical agriculture. Thus, the determination of a representative area or region of the tomographic units (TU) data matrix chosen for CT calibration becomes very important especially during measurements of soil bulk density ( $\rho_b$ ) commonly used as an indicator of soil quality.

In this paper, the importance of a good CT scanner calibration is discussed with emphasis to the best calibration procedure to be chosen to obtain best images in order to determine reliably soil bulk density.

## 2 Materials and Methods

Ten soil clod samples with volumes of the order of 50–100 cm<sup>3</sup> were collected in the 0–15 cm layer of a Rhodic Kandiudalf soil [12], for the determination of  $\rho_b$  by the CT and the conventional gravimetric methodology known as clod method. The soil samples were air-dried up to present constant residual volumetric soil water content. The objective of this procedure was to avoid the influence of water content in the measurements of  $\rho_b$  by the CT method.

Scannings of soil clod samples were obtained with a first generation CT scanner with fixed source-detector arrangement and translation/rotational movements of the samples. The radioactive source used was <sup>241</sup>Am (59.54 keV). NaI(Tl) scintillation crystal (7.62 × 7.62 cm) coupled to a photomultiplier tube was used to detect the monoenergetic photons passing through circular lead collimators of diameters 1 mm between source and sample and 3 mm between sample and detector. The acquired data were stored in a PC and CT images were obtained using the reconstruction algorithm Microvis [13].

The evaluation of photons transmitted along the sample was made in several directions of the same plane for a 2-D image, in different angles called angular steps, until a scan of 180° was completed. In each direction, measurements were taken in different parallel positions separated by a constant distance called linear step. In the present study the soil samples were rotated

over 180° in intervals of 2.25°, with linear movement steps of 0.14 cm.

The TU, which is related to the linear attenuation coefficient ( $\mu_1$ ) of the soil in each crossing position, take the air as the medium with the minimum possible  $\mu_1$  value. In the case of heterogeneous materials like soils, TU is a result of the contributions from solid mineral and organic components, water, and air crossed by the radiation beam, which makes  $\mu_1$  different for each path through the sample. Attenuation of the beam by the air is insignificant as compared with soil particles and water, and it can therefore be neglected. For a soil sample the relation between TU and  $\mu_1$  is given by:

$$\begin{aligned} \text{TU}(E_\gamma) &= \alpha \mu_1(E_\gamma) \\ &= \alpha [\mu_{ms}(E_\gamma) \rho_b + \mu_{mw}(E_\gamma) \theta \rho_w] \end{aligned} \quad (1)$$

where  $E_\gamma$  (keV) is the energy of the gamma photons;  $\alpha$  (cm) is the correlation between  $\mu_1$  of a homogenous material and its respective TU;  $\mu_{ms}$  and  $\mu_{mw}$  (cm<sup>2</sup> g<sup>-1</sup>) are the mass attenuation coefficients of soil and water, respectively; and  $\theta$  (cm<sup>3</sup> cm<sup>-3</sup>) and  $\rho_w$  (g cm<sup>-3</sup>) are the soil volumetric water content and the water density, respectively.

TU differences related to each point of the soil matrix can be associated with differences in gray scales in reconstructed images, considering that the images were reconstructed using a color scheme with an 8-bit resolution. For example, white regions can correspond to points with lower  $\mu_1$  while dark regions to higher. Variations in gray levels correspond to differences in  $\mu_1$  and, consequently, in  $\rho_b$  at each point. It is therefore possible to obtain images that present the density distribution of the sample within the tomographic section. In the case of a moist soil sample, this density distribution includes the water content distribution.

For the calibration of the system  $\mu_1$  was evaluated for selected liquid materials (water, alcohol, and glycerin). The alcohol (C<sub>2</sub>H<sub>5</sub>OH) sample (lot number 30717) manufactured by F. Maia Ind. & Com. Ltda and the glycerin (C<sub>3</sub>H<sub>5</sub>(OH)<sub>3</sub>) sample (lot number 104094) manufactured by Merck presented 99.3% and 87% purity, respectively. They were properly conditioned inside acrylic boxes and then submitted to gamma-ray direct transmission measurements. The very same procedure was followed for the solid (acrylic and nylon) materials. The intensities of monoenergetic photons were taken at three different positions in these materials with  $\mu_1$  representing an arithmetic mean of these measurements. Acrylic and nylon samples used do not present information regarding its homogeneity. Three undisturbed soil samples with different textures were also used in CT calibration. Soils 1, 2, and 3 are: (1) a

sandy clay loam soil (66% sand, 28% clay, and 6% silt), (2) a clay soil (24% sand, 43% clay, and 33% silt), and (3) another clay soil (26% sand, 48% clay, and 26% silt). The laboratory was maintained at constant temperature ( $20 \pm 1$  °C).

The choice of solid samples (nylon, acrylic, and soils) as well as liquid samples (water, alcohol, and glycerin) was in the sense of studying the effect of the use of less homogeneous materials in the evaluation of representative calibrations of first generation tomographs. Some changes of the procedure to obtain the calibration curves (CC) were made in relation to the method originally employed by Crestana et al. [3–5]. A rectangular area with dimensions of  $5 \times 5$  pixels was selected (representing 25 TU values of the CT matrix data) for the determination of a mean TU of the 2-D images obtained by the reconstruction program. Four different positions inside the images were selected for TU evaluation: (1) near the center of the images and (2) at random positions ( $P_2$ ,  $P_3$ , and  $P_4$ ) selected along the images. These choices of different positions, that generate distinct average TU values inside the samples used for calibration, are here called calibration curves when these TU values are correlated with  $\mu_1$ . The total time spent for each CT scan for materials used in calibration was 101 (acrylic), 62 (water), 44 (alcohol), 71 (nylon), 50 (glycerin), and 46 h (soils).

The first CC represents the correlation between  $\mu_1$  and TU of each material for  $P_1$  and the others for  $P_2$ ,  $P_3$ , and  $P_4$ , respectively. TU values for water and alcohol were maintained the very same for each CC. This choice was because these materials were the most homogeneous used in the calibration procedure. For the liquid samples, the selection of the sample position for the evaluation of the mean TU value was made based on the mean value presenting the lowest standard deviation.

The percent deviation between the values of  $\rho_b$  for the four different CCs was calculated according to:

$$PD(\%) = \left| \frac{\rho_b(CC_n) - \rho_b(CC_{n-1})}{\rho_b(CC_n)} \right| \cdot 100 \quad (2)$$

where  $\rho_b(CC_n)$  ( $\text{g cm}^{-3}$ ) is the density value for a specific CC. The subscript  $n$  varies from 1 to 4.

The  $\rho_b$  by CT was calculated by substituting  $\alpha$  of the calibration curve and  $\mu_m$  of water and soil, respectively, in the Beer–Lambert equation. The following equation can be derived to obtain  $\rho_b$ :

$$\rho_b = \frac{\left\{ \left[ \frac{TU(E_\gamma)}{\alpha} \right] - \mu_{mw}(E_\gamma) \cdot \theta_r \rho_w \right\}}{\mu_{ms}(E_\gamma)} \quad (3)$$

**Table 1** Mean values of linear and mass attenuation coefficients for samples utilized to calibrate the gamma-ray CT scanner with 59.54 keV ( $^{241}\text{Am}$ ) energy source radiation

Sample	$\mu_l$ ( $\text{cm}^{-1}$ )	$\rho_b$ ( $\text{g cm}^{-3}$ )	$\mu_m$ ( $\text{cm}^2 \text{g}^{-1}$ )
Acrylic	$0.1411 \pm 0.0009$	$0.93^a$	$0.1517 \pm 0.0010$
Water	$0.1989 \pm 0.0002$	$0.99^a$	$0.2001 \pm 0.0004$
Alcohol	$0.1475 \pm 0.0005$	$0.77^a$	$0.1916 \pm 0.0006$
Glycerin	$0.2197 \pm 0.0006$	$1.20^a$	$0.1831 \pm 0.0005$
Nylon	$0.2051 \pm 0.0013$	$1.12^a$	$0.1831 \pm 0.0012$
Soil 1	$0.3888 \pm 0.0047$	$1.56 \pm 0.02^b$	$0.2492 \pm 0.0030$
Soil 2	$0.5306 \pm 0.0046$	$1.59 \pm 0.04^b$	$0.3339 \pm 0.0029$
Soil 3	$0.4076 \pm 0.0045$	$1.33 \pm 0.05^b$	$0.3065 \pm 0.0034$

<sup>a</sup>Density values obtained without repetitions.

<sup>b</sup> $\rho_b$  determined by the volumetric ring method are an arithmetic mean value of five repetitions

where  $\theta_r$  represents the air dry volumetric soil water content of the sample before CT scanning.

For the evaluation of  $\mu_{1s}$  air-dried soil was passed through a 2.0-mm sieve and packed as homogeneously as possible into a thin wall acrylic container ( $4.9 \times 5.1 \times 5.5 \text{ cm}^3$ ). The intensities of monoenergetic photons were measured at five different positions in the soil sample with  $\mu_{1s}$  representing an arithmetic mean of these measurements. In order to obtain  $\mu_m$  of water and soil it was measured the densities of these materials by the division of their mass and the internal volume occupied by them.

Some statistical parameters were used to evaluate equipment calibration: homogeneity, sensibility and the intrinsic errors of the technique coming from the statistics of gamma-ray source emission. To verify the data homogeneity obtained by CT some basic statistical analyses were performed. Mean, standard deviation, and the coefficient of variation of data matrix con-

**Table 2** Soil bulk density error ( $E_{\rho_b}$ ) due to the equipment considering the different materials used for the calibration curve (CC) evaluation

Sample	$E_{\rho_b}$ ( $\text{g cm}^{-3}$ ) <sup>a</sup>			
	CC <sub>1</sub>	CC <sub>2</sub>	CC <sub>3</sub>	CC <sub>4</sub>
Acrylic	0.160	0.150	0.154	0.154
Water	0.051	0.048	0.049	0.049
Alcohol	0.056	0.052	0.053	0.054
Glycerin	0.068	0.064	0.065	0.065
Nylon	0.056	0.052	0.053	0.054
Soil 1	0.101	0.095	0.098	0.098
Soil 2	0.155	0.146	0.149	0.150
Soil 3	0.198	0.186	0.190	0.191

<sup>a</sup>For the evaluation of ( $E_{\rho_b}$ ) were considered the following CVs for each material used in CT calibration: 9.8% (acrylic), 3.1% (water), 3.4% (alcohol), 3.4% (nylon), 4.1% (glycerin), 6.2% (soil 1), 9.5% (soil 2), and 12.1% (soil 3). CVs selected for acrylic, nylon, glycerin, and soils were obtained considering the data matrix for the entire samples

taining 25 selected values of TU for different sample positions were calculated. The sensibility of the equipment was also tested changing the TU in steps of one unit for a mean constant value of the volumetric soil clod water content ( $\theta = 0.01 \text{ cm}^3 \text{ cm}^{-3}$ ). The error attributed to the equipment was determined applying the CV obtained for each used material to the mean values of TU of the soil samples.

### 3 Results and Discussion

Mean attenuation coefficients of the materials used for CT calibration are presented in Table 1. The mean

mass attenuation coefficient obtained for the soil clod was  $0.3390 \pm 0.0020 \text{ cm}^2 \text{ g}^{-1}$ , which agree with values found in the literature for the  $^{241}\text{Am}$  radiation [14]. The denser materials used for CT calibration were the soil samples, which presented the higher values of  $\mu_1$ . This result can be explained by the value of soil particle densities for the soil samples ( $2.55 \text{ g cm}^{-3}$  for soil 1,  $2.68 \text{ g cm}^{-3}$  for soil 2, and  $2.54 \text{ g cm}^{-3}$  for soil 3).

In the analysis of sample homogeneity CV values of 3.1% and 3.4% were obtained for the water and alcohol samples, respectively. The other samples presented CV values that varied according to the selected position used to obtain the mean value of TU (rectangular area of  $5 \times 5$  pixels) in the data matrix. The acrylic sample

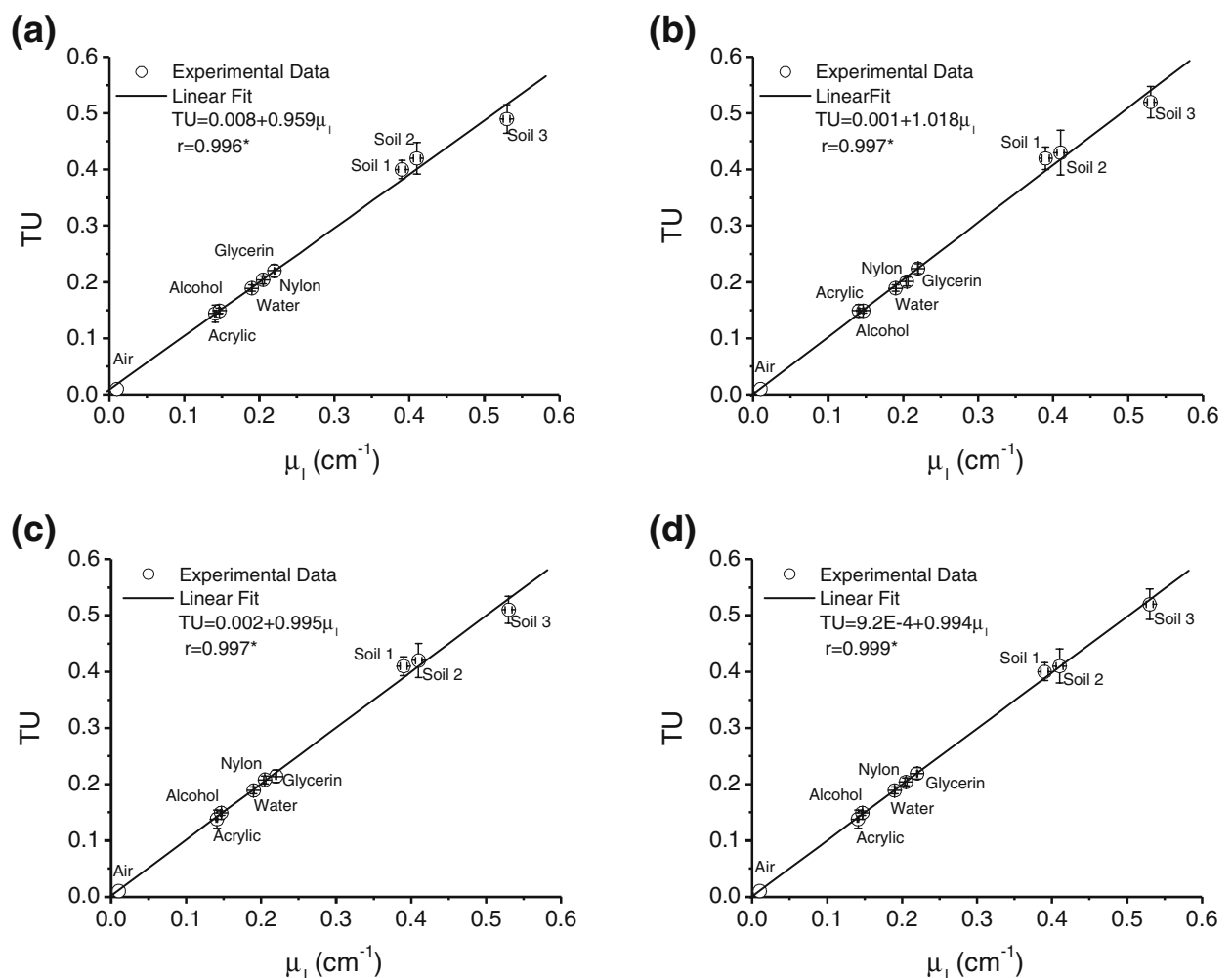


**Fig. 1** Computed tomography (CT) calibration curves for  $^{241}\text{Am}$  gamma-ray photons. Tomographic units (TU) and  $\mu_1$  represent the tomographic unit and the linear attenuation coefficient, respectively. **a** calibration curve 1 (CC<sub>1</sub>), **b** CC<sub>2</sub>, **c** CC<sub>3</sub>, and **d** CC<sub>4</sub>.

The correlation between TU and  $\mu_1$  for air was obtained for simulated values of these two terms. The error bars for TU and  $\mu_1$  represent the standard deviation of the measurements

presented variations in CV from 10.4% to 11.6%, the glycerin sample from 4.0% to 5.1%, and the nylon sample from 3.4% to 4.0%. Soil samples 1, 2, and 3

presented variations in CV from: 3.7% to 10.1%, 5.2% to 11.1%, and 9.8% to 17.5%, respectively.

For the more homogeneous materials the variations in TU can be attributed mainly to the statistic variations of the  $^{241}\text{Am}$  decay process and for the long total time spent to perform the CT scans [15, 16]. The later has great importance when changes in photopeak position occur. The higher CV values obtained for the other samples can also be associated to impurities of the materials, to the dimensions of the samples used for the determination of the attenuation coefficients, also to the long total time for complete CT scan, and to artifacts in the tomographic images [1, 15, 17].

Short counting time or the low gamma-ray source activity which results in low gamma beam intensities and consequently poor counting statistics also represent source of errors. A possible solution for this problem could be the use of a more appropriate or more intense radioactive source. Another alternative could be the use of higher counting times but this would result in a very high sample scanning time that could amplify the variations due to fluctuations in the spectrum position during the data acquisition as discussed earlier.

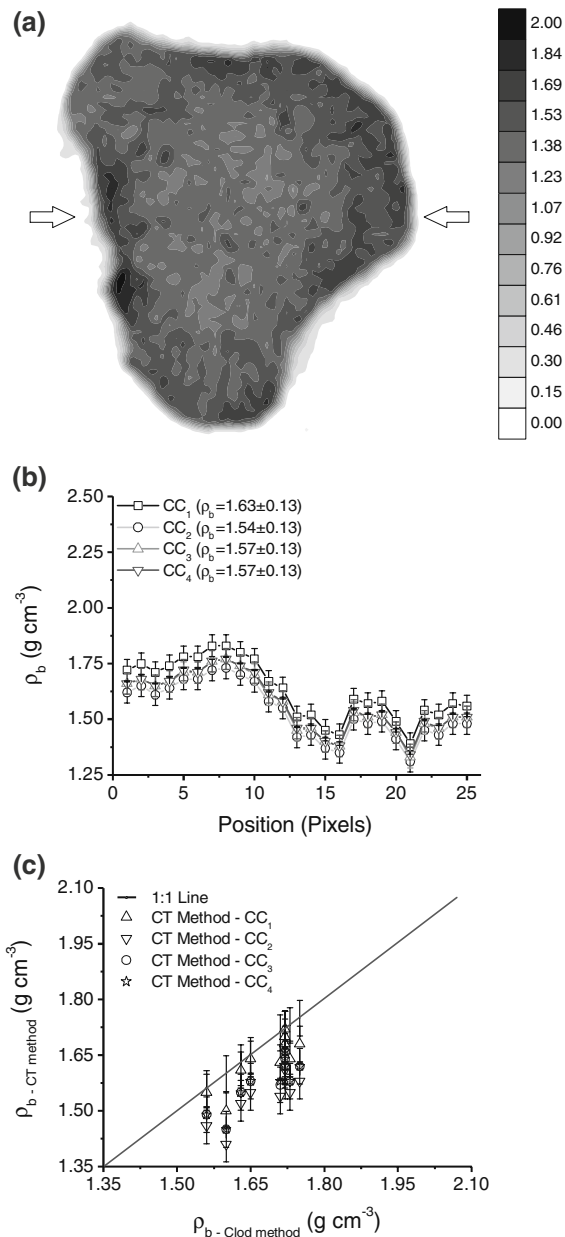
Another procedure could be the use of collimators with larger diameters to improve the gamma beam intensities maintaining short counting times. However in this case the increase in the detection of scattered photons could cause other worse consequences [1, 18].

Table 2 shows the results of the calculated errors due to the tomograph system in  $\rho_b$  determinations when taking different materials for the equipment calibration.

The value determined for the sensibility of the system was of  $0.003 \text{ g cm}^{-3}$  per unit TU. Analyzing the errors of the system according to Table 2, it can be observed that the average was of  $0.154 \text{ g cm}^{-3}$  for the acrylic sample,  $0.049 \text{ g cm}^{-3}$  for water,  $0.054 \text{ g cm}^{-3}$  for alcohol,  $0.054 \text{ g cm}^{-3}$  for nylon,  $0.065 \text{ g cm}^{-3}$  for glycerin,  $0.098 \text{ g cm}^{-3}$  for soil 1,  $0.150 \text{ g cm}^{-3}$  for soil 2, and  $0.191 \text{ g cm}^{-3}$  for soil 3. The errors obtained in soil  $\rho_b$  measurements indicate that the samples of water, nylon, and alcohol are the most homogeneous. For example, the use of the acrylic sample induces an error of about  $0.15 \text{ g cm}^{-3}$  in the measurement of the soil  $\rho_b$ . The error obtained for water is in accordance to the results obtained by Pedrotti et al. [19].

Combining the several mean TUs evaluated for the materials utilized in the system calibration, it was possible to obtain four calibration curves for the  $^{241}\text{Am}$  gamma-ray source (Fig. 1).

The statistical analysis of the regression showed that there is a high positive linear correlation ( $P < 0.05$ ) between  $\mu_1$  and TU for all the calibration curves.



**Fig. 2** 2-D tomographic images of a clod sample used to evaluate the soil bulk density ( $\rho_b$ ). Arrows indicate the position of the transect used for  $\rho_b$  variation analysis inside the clod sample. The scale represents the  $\rho_b$  distribution. **b** Variation in  $\rho_b$  of the clod sample for the different calibration curves (CC) obtained for the transect showed in **a**. Experimental data variations were obtained considering only one line of the TU matrix. **c** Correlation between CT and gravimetric  $\rho_b$  (clod method) measurements using the four CCs obtained. The error bars for items **b** and **c** represent the system error taking the water as the reference



**Table 3** Mean values of soil bulk density ( $\rho_b$ ) evaluated using different computed tomography (CT) calibration curves (CC) for clod samples

	$\rho_b$ (g cm <sup>-3</sup> )			
	CC <sub>1</sub>	CC <sub>2</sub>	CC <sub>3</sub>	CC <sub>4</sub>
Clod <sup>a</sup>	1.64 ± 0.08	1.54 ± 0.07	1.58 ± 0.07	1.58 ± 0.07
PDclod (%) <sup>b</sup>	0.0	5.7	3.6	3.5

<sup>a</sup>  $\rho_b$  determined by CT are an arithmetic mean value of ten repetitions.

<sup>b</sup> PD is the percentual deviation of  $\rho_b$  calculated in relation to the best CC, being in the case of this study CC<sub>1</sub> (considering the reference for this choice the value of  $\rho_b$  obtained by the clod method (1.68 g cm<sup>-3</sup>))

However, the slopes ( $\alpha$ ) of the calibration curves are different which result in different estimates of  $\rho_b$  by (3).

The CT image (Fig. 2a) obtained from transverse sections and the available data allowed a continuous 2-D analysis of TU distributions and, consequently, of  $\rho_b$  variations along the sample (Fig. 2b).

Through the analysis of the density profiles (Fig. 2b) for the four CCs it is possible to observe small differences in the  $\rho_b$  profiles. However, the density variations along the positions for the different calibrations remain the same once only the parameter  $\alpha$  is

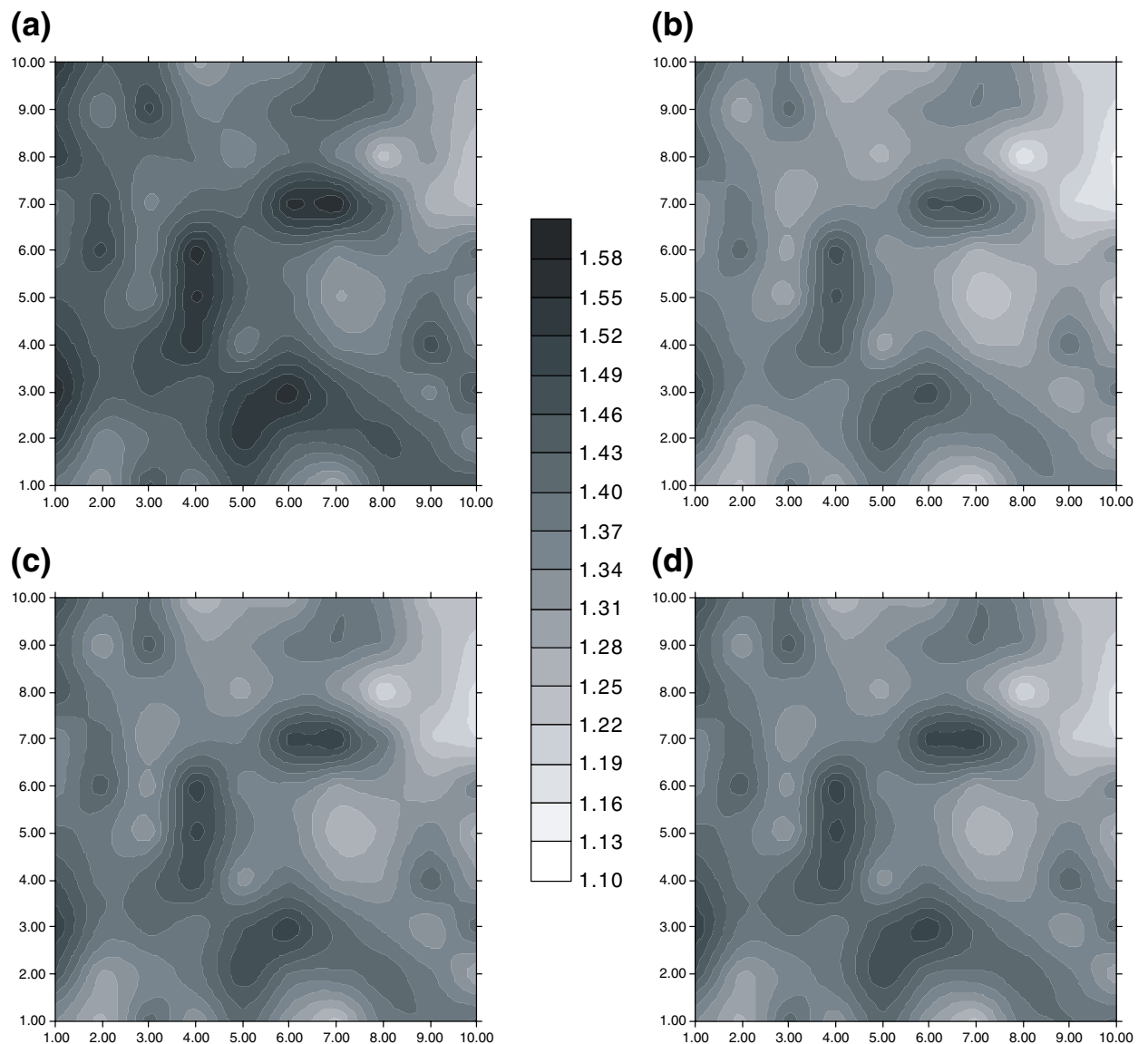


**Fig. 3** Maps of soil bulk density ( $\rho_b$ ) obtained using the different calibration curves: **a** calibration curve 1 (CC<sub>1</sub>), **b** CC<sub>2</sub>, **c** CC<sub>3</sub>, and **d** CC<sub>4</sub>. The gray scale shows the  $\rho_b$  range values

changed in (3). Thus, as  $\alpha$  is distinct for each CC and inversely proportional to TU, increases in this parameter cause decreases in  $\rho_b$  values. This result demonstrates the need of good calibration curves to evaluate reliably soil physical properties.

Taking the water as the reference, which presented the highest homogeneity (CV = 3.1%) and the mean value of  $\rho_b$  as  $1.60 \text{ g cm}^{-3}$  (Fig. 2b) for the soil, it can be observed that  $\rho_b$  can vary from about  $1.55\text{--}1.65 \text{ g cm}^{-3}$ . This result shows that the  $\rho_b$  values are not in the range of the system error only for CC<sub>2</sub>. Therefore, the use of CC<sub>2</sub> to evaluate  $\rho_b$  will not give representative values of this soil physical property.

When the soil samples are not considered in the CT calibration the slope ( $\alpha$ ) of the CCs become: 0.959 for CC<sub>1</sub> ( $r = 0.999$ ), 0.952 for CC<sub>2</sub> ( $r = 0.993$ ), 0.979 for CC<sub>3</sub> ( $r = 0.995$ ), and 0.999 for CC<sub>4</sub> ( $r = 0.999$ ). Considering the last CCs, the water as the reference material, and the mean value of  $\rho_b$  as  $1.61 \text{ g cm}^{-3}$  for the soil, it can be observed that  $\rho_b$  can vary from  $1.56$  to  $1.66 \text{ g cm}^{-3}$ . The value of  $\rho_b$  obtained by using the last CCs varied from  $1.58$  to  $1.63 \text{ g cm}^{-3}$ . This result for this specific case shows that the  $\rho_b$  values are in the range of the system error independently of the calibration adopted. Therefore, even using samples with CV in the order of 10% (glycerin) the results of  $\rho_b$  would be within the error range of the system. On the other hand, the use of samples with higher CV variations (soils) can give results of  $\rho_b$  not representative depending on the CC adopted.

Results of correlation between CT and gravimetric bulk density measurements for the clod sample for the four calibration curves (Fig. 2c) show that  $\rho_b$  measured from CC<sub>1</sub> presented the best correlations in relation to  $\rho_b$  determined by the clod method. Practically, all  $\rho_b$  values obtained by the CT method were lower than that obtained by the clod method.

Table 3 presents mean values of  $\rho_b$  and the percent deviation in relation to CC<sub>1</sub>, which was chosen as the best calibration curve, since it presented  $\rho_b$  values closer to the conventional method. The mean  $\rho_b$  obtained by CT for CC<sub>1</sub> is in line with those evaluated by Timm et al. [20] for the same type of soil using the clod method.

Finally, the maps of  $\rho_b$  distributions (Fig. 3) in a selected matrix of 100 values of TU ( $10 \times 10$  pixels) positioned in the central region of the clod image (Fig. 2a), show the differences in  $\rho_b$  configuration when distinct CCs are used.

The different  $\rho_b$  maps obtained show that depending on the calibration curve important changes are observed in the maps of distribution of this soil property. This result can be very important when studies related

to spatial and temporal variability of  $\rho_b$  are being carried out in agricultural management projects.

## 4 Conclusions

In summary, the results obtained in this study show that although it is important to choose homogeneous materials for the calibration of first generation tomographic systems aiming to obtain representative values of  $\rho_b$ , the statistical error involved in the gamma source photon emission can be of such an order that even using a material with high CV (in the order of 10%) for the calibration of the system, the  $\rho_b$  average value obtained with different CCs can be within the range of the error of the CT system.

However, if the interest is, for example, to compare the effects of soil compaction on soil sample structure using  $\rho_b$  determined by tomography, the choice of different calibration curves will provide results that can lead to ambiguous interpretation.

**Acknowledgements** The authors are grateful to Conselho Nacional de Desenvolvimento Científico e Tecnológico (CNPq) for PQ grants and to Fundação Araucária (protocol no. 10198), Fundo Paraná/SETI and Governo do Paraná for financial support.

## References

1. A.C. Kak, M. Slaney, *Principles of Computerized Tomographic Imaging* (IEEE Press, New York, 1988), 327 pp
2. V. Clausnitzer, J.W. Hopmans, *Adv. Water Res.* **22**, 577 (1999)
3. S. Crestana, S. Mascarenhas, R.S. Pozzi-Mucelli, *Soil Sci.* **140**, 326 (1985)
4. S. Crestana, R. Cesareo, S. Mascarenhas, *Soil Sci.* **142**, 56 (1986)
5. S. Crestana, P.E. Cruvinel, C.M.P. Vaz, R. Cesareo, S. Mascarenhas, K. Reichardt, *Rev. Bras. Cienc. Solo* **16**, 161 (1992)
6. V.K. Phogat, L.A.G. Aylmore, *Aust. J. Soil Res.* **27**, 313 (1989)
7. A. Macedo, S. Crestana, C.M.P. Vaz, *Soil Tillage Res.* **49**, 249 (1998)
8. D. Jégou, J. Brunotte, H. Rogasik, Y. Capowicz, H. Diestel, S. Schrader, D. Cluzeau, *Soil Biol.* **38**, 329 (2002)
9. L.F. Pires, R.J.C. Arthur, O.O.S. Bacchi, K. Reichardt, *Nucl. Instrum. Methods Phys. Res. B* **259**, 969 (2007)
10. L.F. Pires, R.C.J. Arthur, V. Correchel, O.O.S. Bacchi, K. Reichardt, R.P. Camponez do Brasil, *Braz. J. Phys.* **34**, 728 (2004)
11. J.M. Oliveira, F.Z.C. Lima, J.A. Milito, A.C.G. Martins, *Braz. J. Phys.* **35**, 789 (2005)
12. Soil Survey Staff, *Soil taxonomy. A basic system of soil classification for making and interpreting soil surveys. USDA Natural Resources Conservation Service Agricultural Handbook 436* (US Gov. Printing Office, Washington, 1999)



13. Microvis, *Programa de Reconstrução e Visualização de Imagens Tomográficas, Guia do Usuário* (EMBRAPA/CNPDIA, São Carlos, 2000)
14. C.M.P. Vaz, J.M. Naime, A. Macedo, *Soil Sci.* **164**, 403 (1999)
15. E.S.B. Ferraz, R.S. Mansell, *Determining water content and bulk density of soil by gamma-ray attenuation methods* (IFAS, Florida, 1979), 51 pp
16. W.H. Gardner, G.S. Campbell, C. Calissendorff, *Soil Sci. Soc. Am. Proc.* **36**, 393 (1972)
17. M.A. Abdel-Rahman, E.A. Badawi, Y.L. Abdel-Hady, N. Kamel, *Nucl. Instrum. Methods Phys. Res. A* **447**, 432 (2000)
18. G.S. Sidhu, K. Singh, P.S. Singh, G.S. Mudahar, *Rad. Phys. Chem.* **56**, 535 (1999)
19. A. Pedrotti, E.A. Pauletto, S. Crestana, P.E. Cruvinel, C.M.P. Vaz, J.M. Naime, A.M. Silva, *Pesq. Agropec. Bras.* **38**, 819 (2003)
20. L.C. Timm, L.F. Pires, K. Reichardt, R. Roveratti, J.C.M. Oliveira, O.O.S. Bacchi, *Aust. J. Soil Res.* **43**, 97 (2005)